

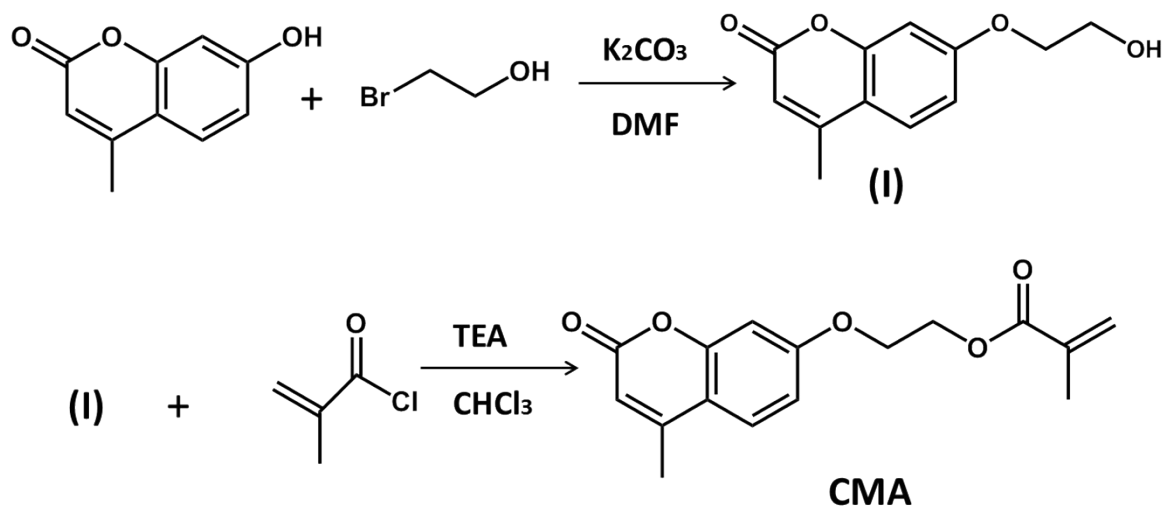
## SUPPORTING INFORMATION

### **Triply responsive coumarin-based microgels with remarkably large photo-switchable swelling**

Dongdong Lu<sup>a,\*</sup>, Mingning Zhu<sup>a</sup>, Shanglin Wu<sup>a</sup>, Wenkai Wang<sup>a,b</sup>, Qing Lian<sup>a</sup> and Brian R. Saunders<sup>a,\*</sup>

<sup>a</sup>*School of Materials, University of Manchester, MSS Tower, Manchester, M13 9PL, U.K.*

<sup>b</sup>*Beijing National Laboratory for Molecular Sciences (BNLMS), College of Chemistry and Molecular Engineering, Peking University, Beijing 100871, China*



**Scheme S1.** Synthesis of 7-(2-methacryloyloxyethoxy)-4-methylcoumarin (CMA). The precursor, (I), is 7-(2-hydroxyethoxy)-4-methylcoumarin.

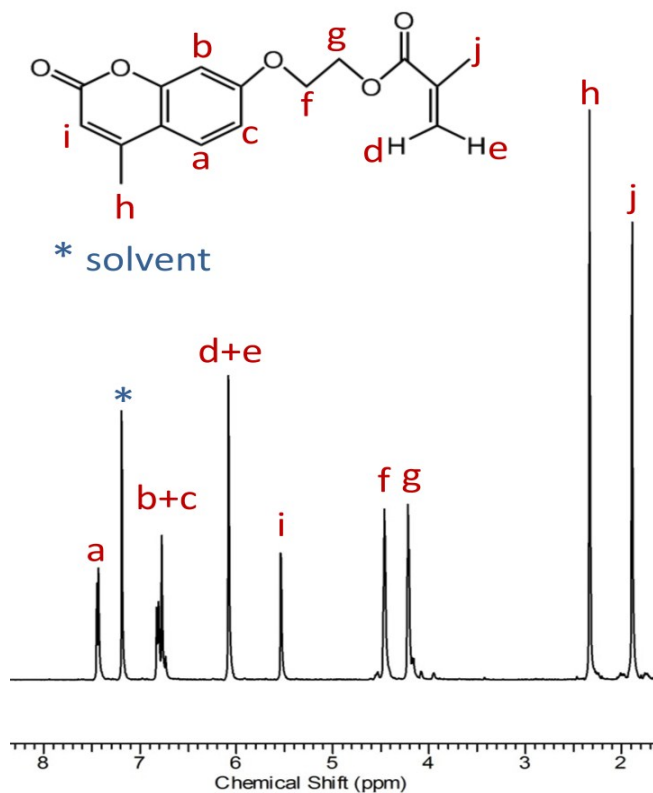


**Figure S1.** <sup>1</sup>H NMR spectrum and assignments for CMA. The peak labelled with an asterisk is due to solvent (CDCl<sub>3</sub>). The peak positions and integrations confirmed the identify and high purity (95%) of CMA.

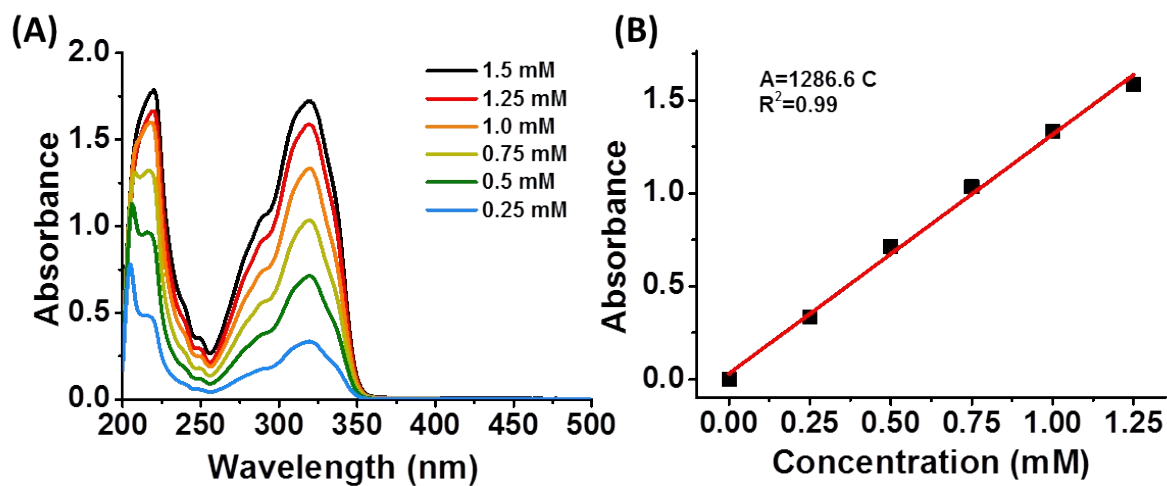


**Figure S2.** (A) UV-visible spectra for CMA at various concentrations in methanol. (B) Variation of absorbance at 320 nm with CMA concentration. The molar extinction coefficient was calculated from (B) as  $1286.6 \text{ mol}^{-1} \text{ dm}^3 \text{ cm}^{-1}$ .

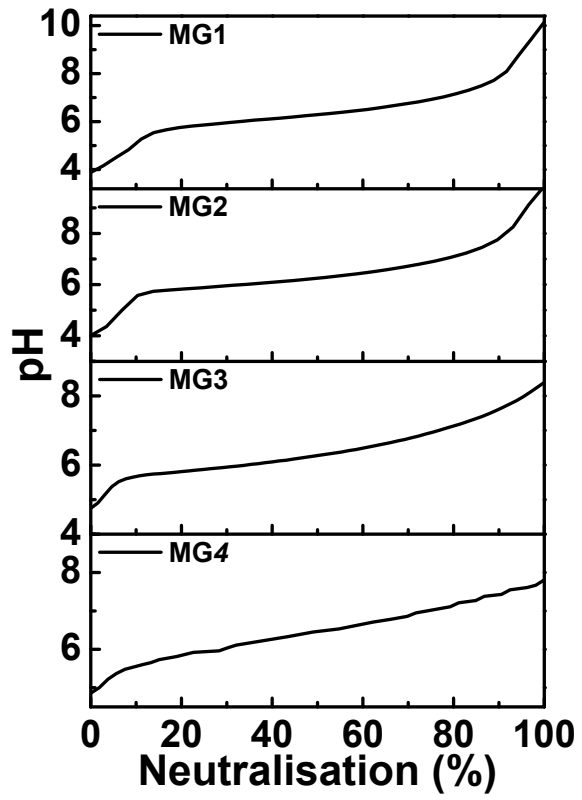
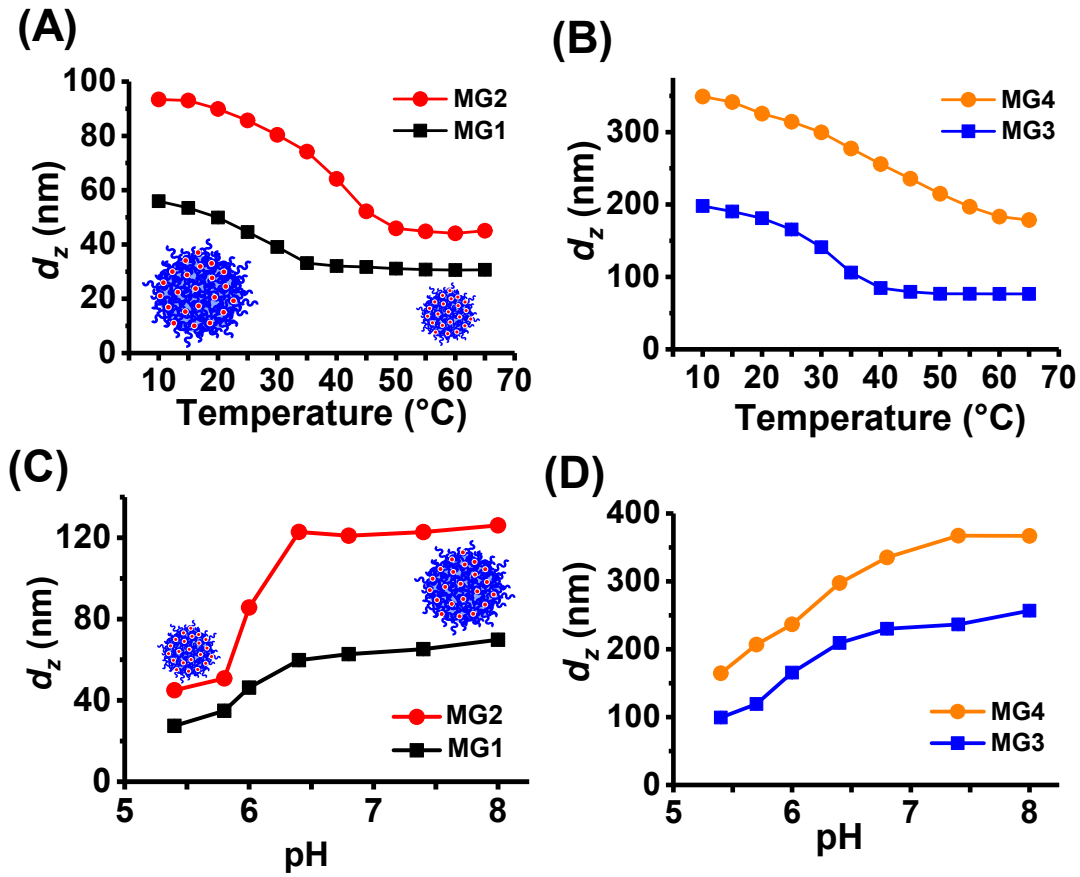


Figure S3. Titration data for all the microgels studied.

## Temperature- and pH-responsive properties of the as-made, non-irradiated microgels

Variable temperature dynamic light scattering (DLS) data for the as-made, non-irradiated, microgel dispersions measured at pH 6.0 are shown in Fig. S4A and S4B. The  $d_z$  values decreased by a factor of  $\sim 2$  when the temperature was increased from 10 to 60 °C and the size distributions remained monomodal (see Fig. S5). The variations of  $d_z$  with pH were measured at 25 °C for MG1 and MG2 (see Fig. S4C). Data for the MG3 and MG4 systems are shown in Fig. S4D. The  $d_z$  values increased strongly as the pH approached the respective apparent  $pK_a$  values (of 5.9 – 6.2, Table 1) due to increasing electrostatic repulsion between  $-\text{COO}^-$  groups. The DLS size distributions remained monomodal with no evidence of particle fragmentation as the pH increased (Fig. S6). The suggestion that electrostatic repulsion caused swelling is supported by electrophoretic mobility measurements for MG4 where the values became increasingly negative as the pH increased (see Fig. S7, ESI†). (Mobility is reported rather than zeta potential because microgel particles do not have a well-defined surface.) It is interesting that the microgels did not disassemble when the pH was increased (Fig. S6) despite the fact that no crosslinking monomer was used during preparation. Self-crosslinking is not possible for methacrylate monomers<sup>1</sup>. Consequently, this result is attributed to polymer chain entanglement as well as reversible photodimerization and cleavage through two-photon absorption of visible light of coumarins<sup>2</sup>. Even though we protected the MG dispersion from visible light as much as possible, some light exposure was inevitable during synthesis.



**Figure S4.** Temperature responsive properties for as-made (non-irradiated) (A) MG1 and MG2 and (B) MG3 and MG4 dispersions. The data in (A) and (B) were measured at pH 6.0. The pH-responsive properties are also shown for (C) MG1 and MG2 and (D) MG3 and MG4 dispersions. The data in (C) and (D) were measured at 25  $^{\circ}\text{C}$ .

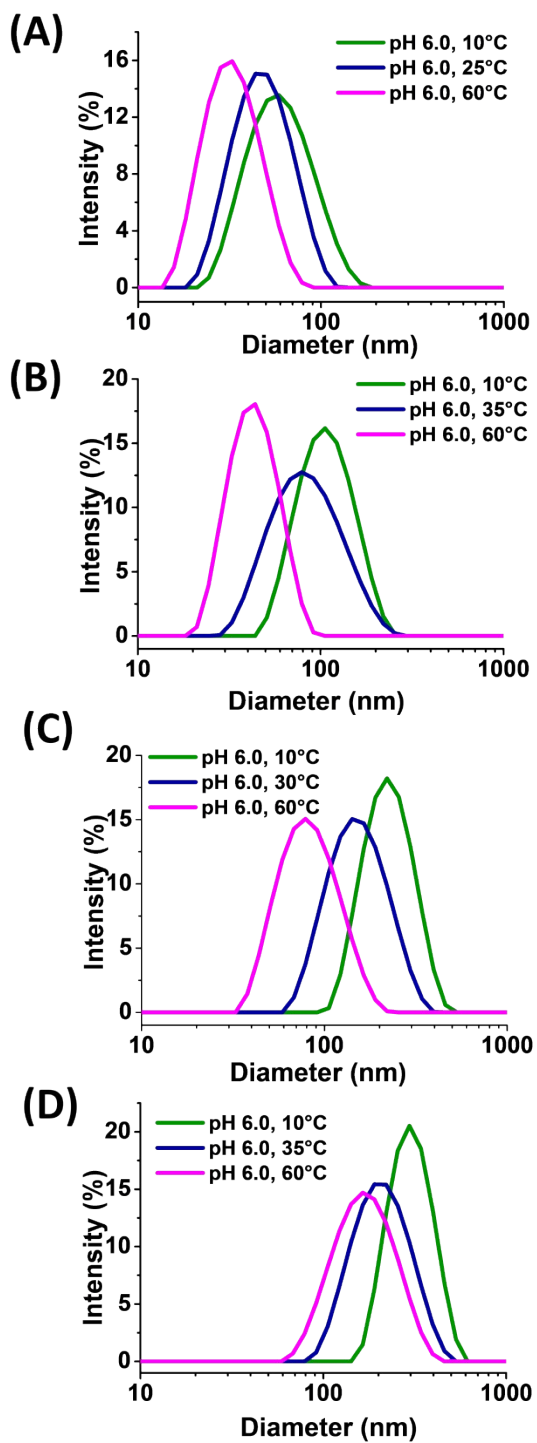


**Figure S5** DLS size distributions for as-made (non-irradiated) MG1 (A), MG2 (B), MG3 (C) and MG4 (D) measured at different temperatures. The pH was 6.0.



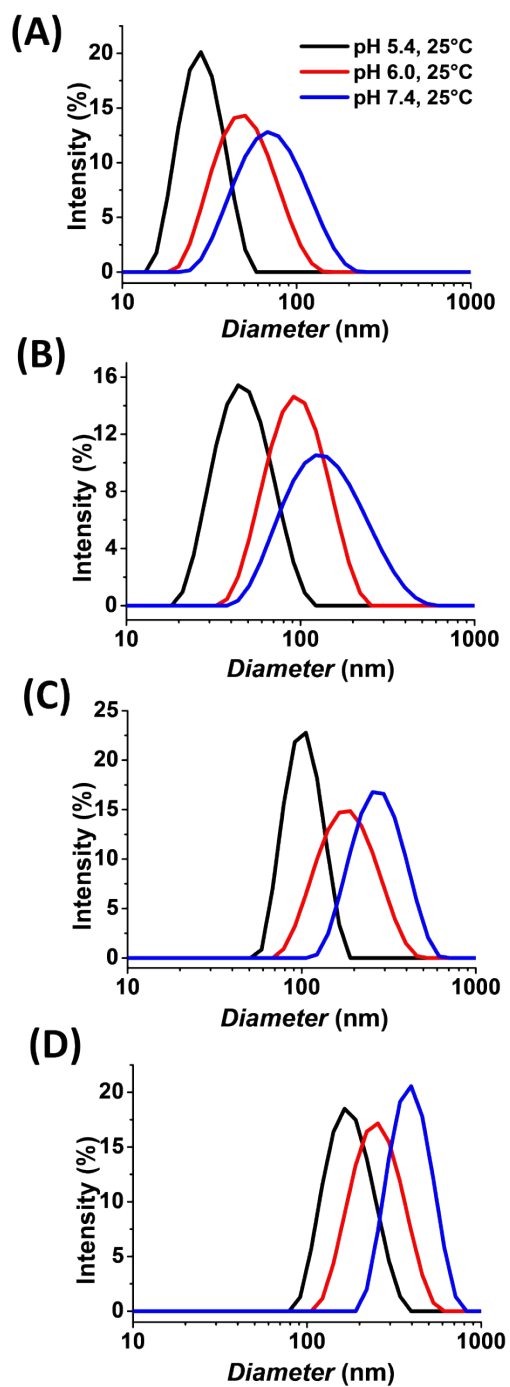


**Figure S6.** DLS size distributions for as-made (non-irradiated) MG1 (A), MG2 (B), MG3 (C) and MG4 (D) measured at different pH values. The temperature was 25 °C. The scale in (A) applies to all graphs.

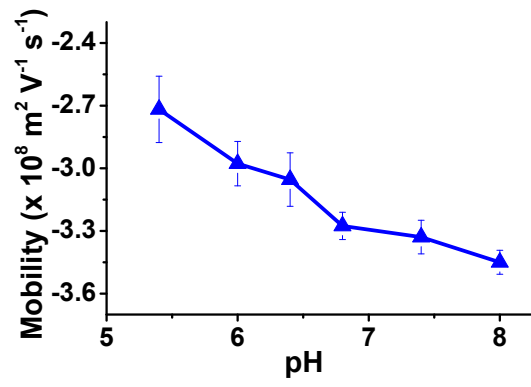


**Figure S7.** Variation of electrophoretic mobility with pH for as-made (non-irradiated) MG4 at 25 °C.

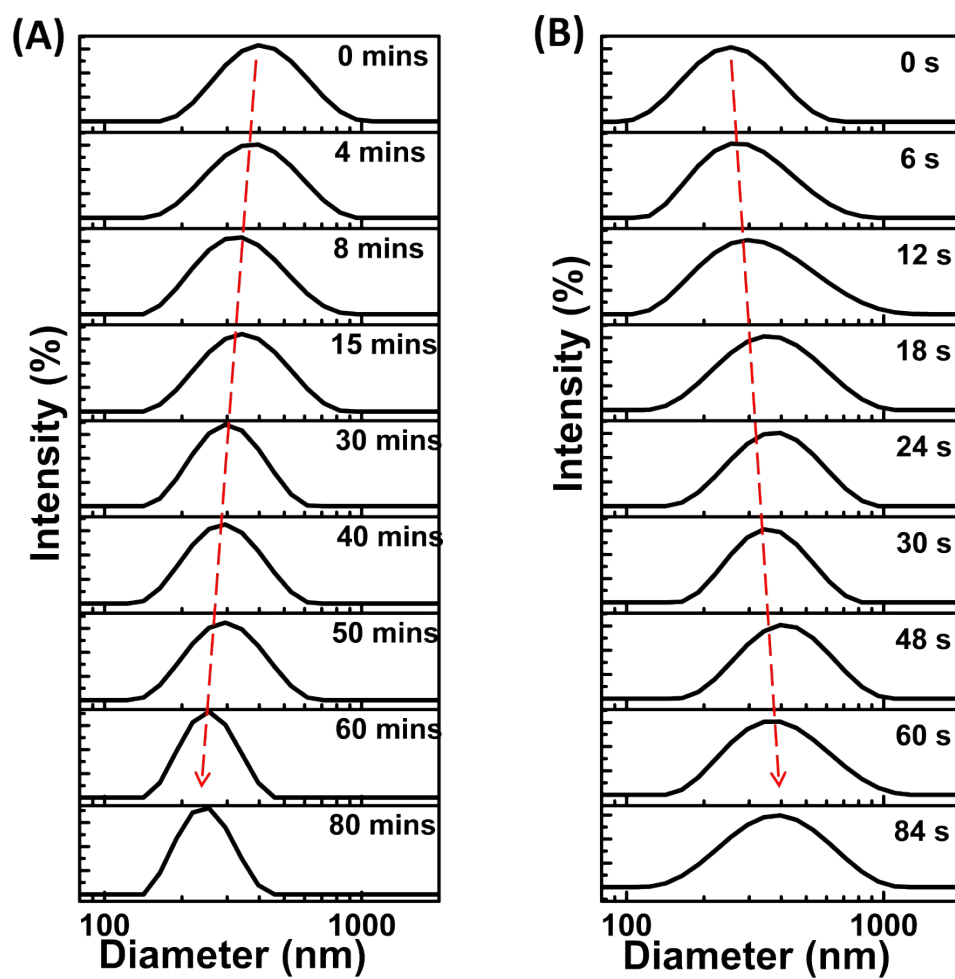


**Figure S8.** DLS size distributions measured for MG4 during (A) photo-crosslinking using 365 nm irradiation and (B) photo-de-crosslinking using 254 nm irradiation. The data were measured at pH 7.4 and 25 °C. The dotted lines highlight the changes that occurred.

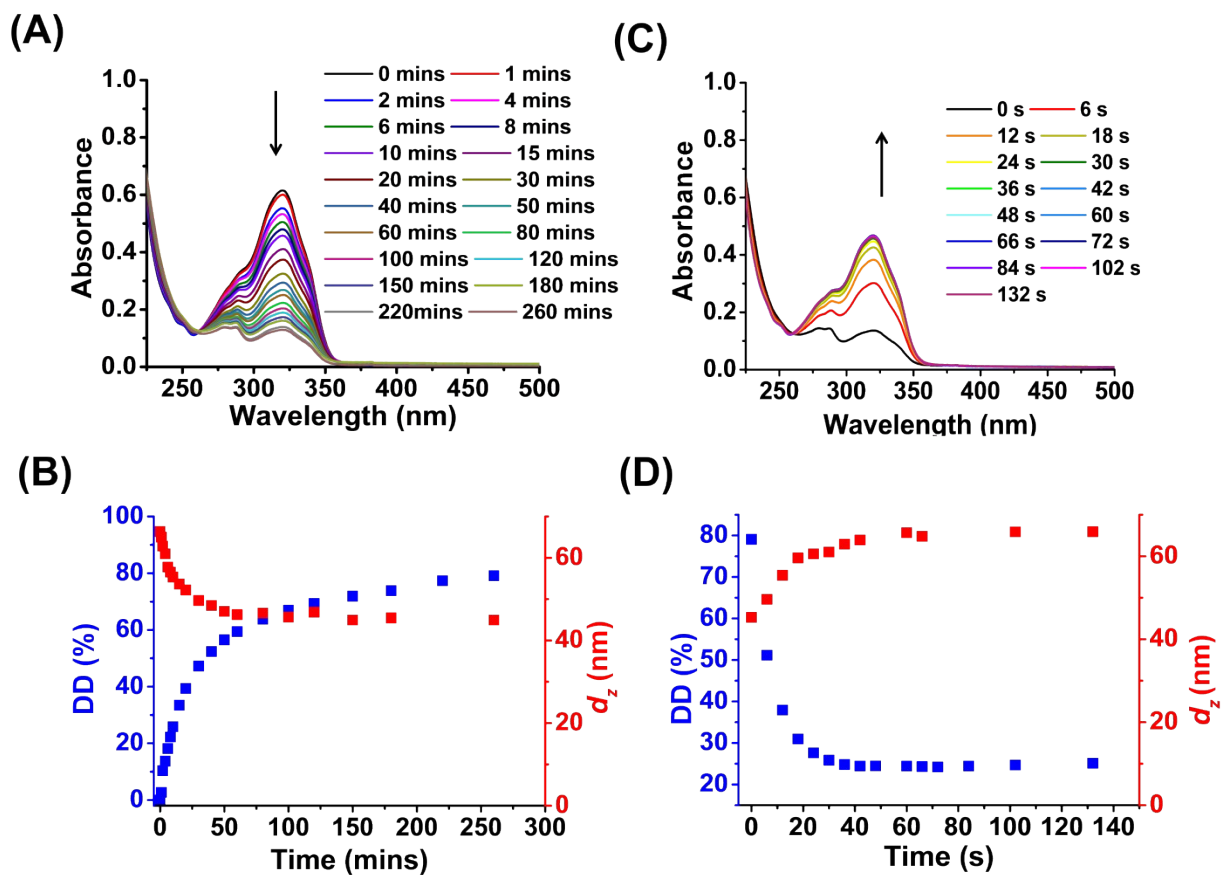


**Figure S9.** UV-visible spectra of MG1 during (A) photo-crosslinking at 365 nm and (B) variation of  $d_z$  and DD with time. (C) UV-visible spectra measured during photo-decrosslinking at 254 nm and (D) variation of  $d_z$  and DD with time. The pH and temperature used to obtain the  $d_z$  data were 7.4 and 25 °C.

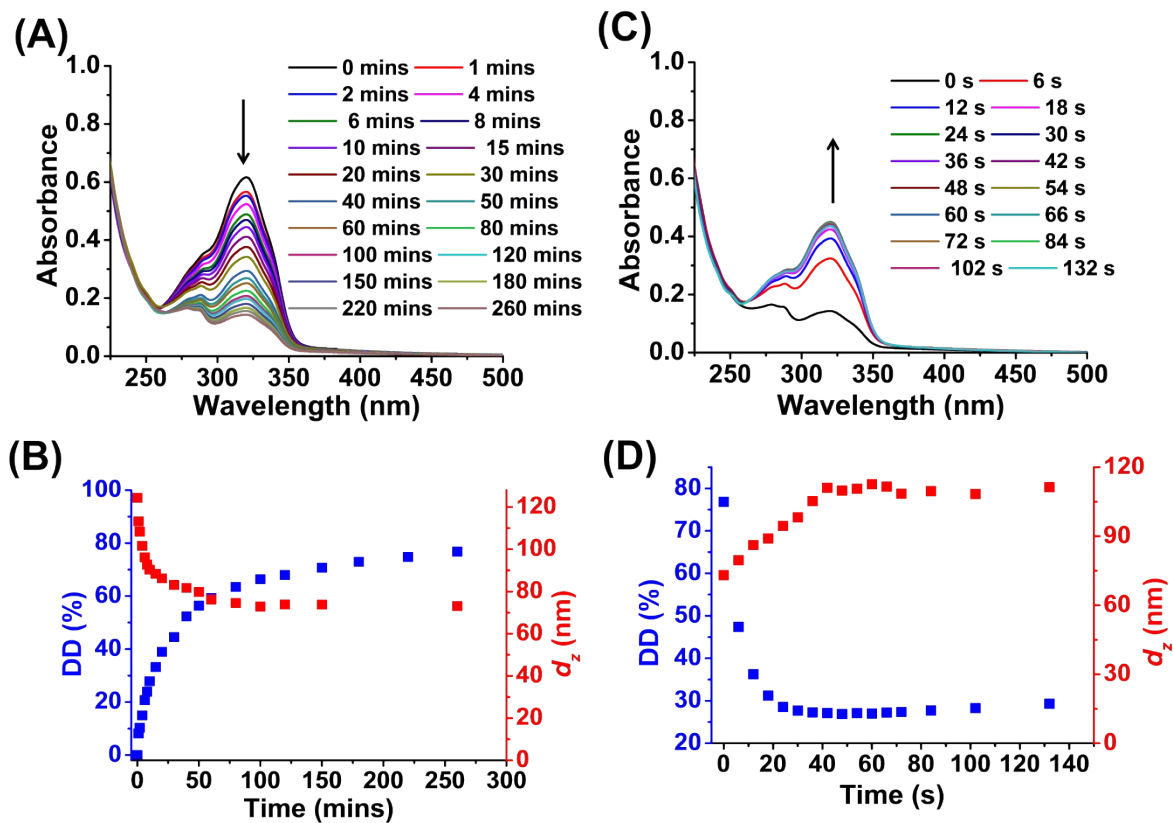


**Figure S10.** UV-visible spectra of MG2 during (A) photo-crosslinking at 365 nm and (B) variation of  $d_z$  and DD with time. (C) UV-visible spectra measured during photo-decrosslinking at 254 nm and (D) variation of  $d_z$  and DD with time. The pH and temperature used to obtain the  $d_z$  data were 7.4 and 25 °C.

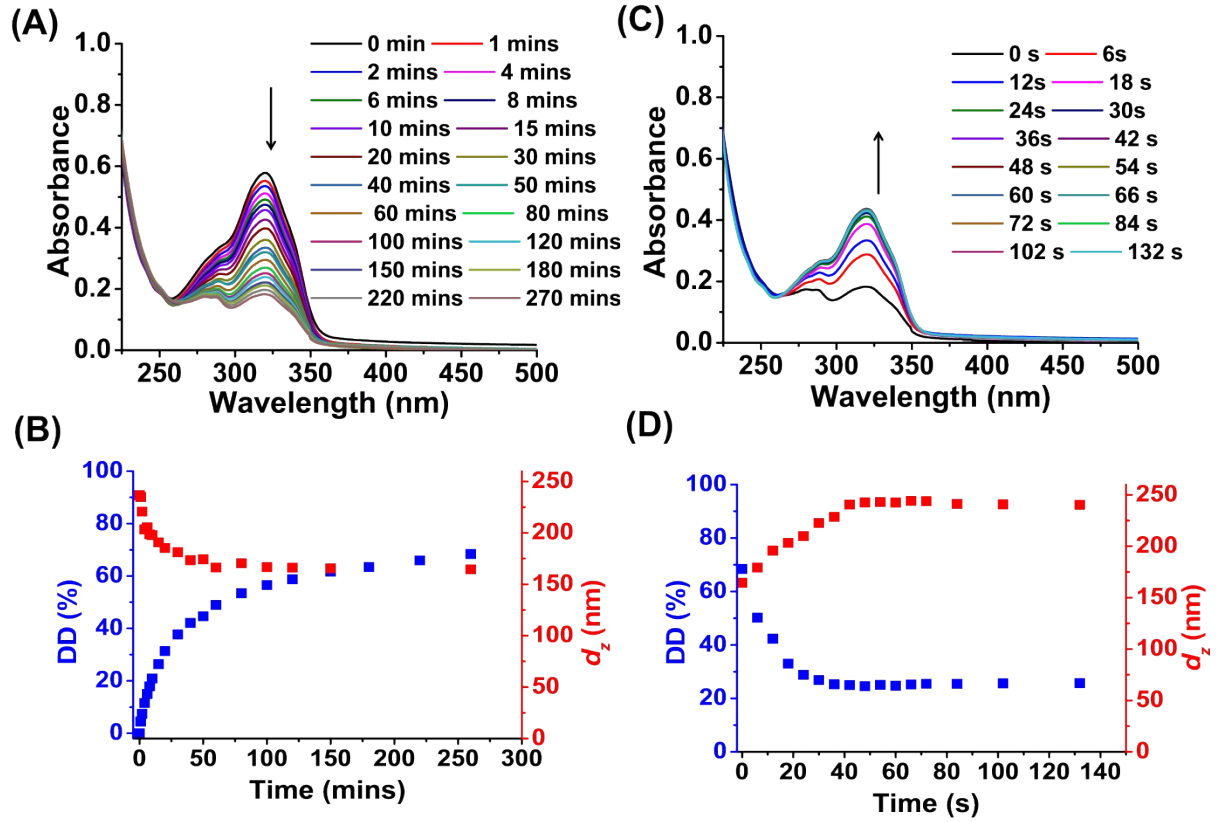


**Figure S11.** UV-visible spectra of MG3 during (A) photo-crosslinking at 365 nm and (B) variation of  $d_z$  and DD with time. (C) UV-visible spectra measured during photo-decrosslinking at 254 nm and (D) variation of  $d_z$  and DD with time. The pH and temperature used to obtain the  $d_z$  data in (A) to (D) were 7.4 and 25 °C.

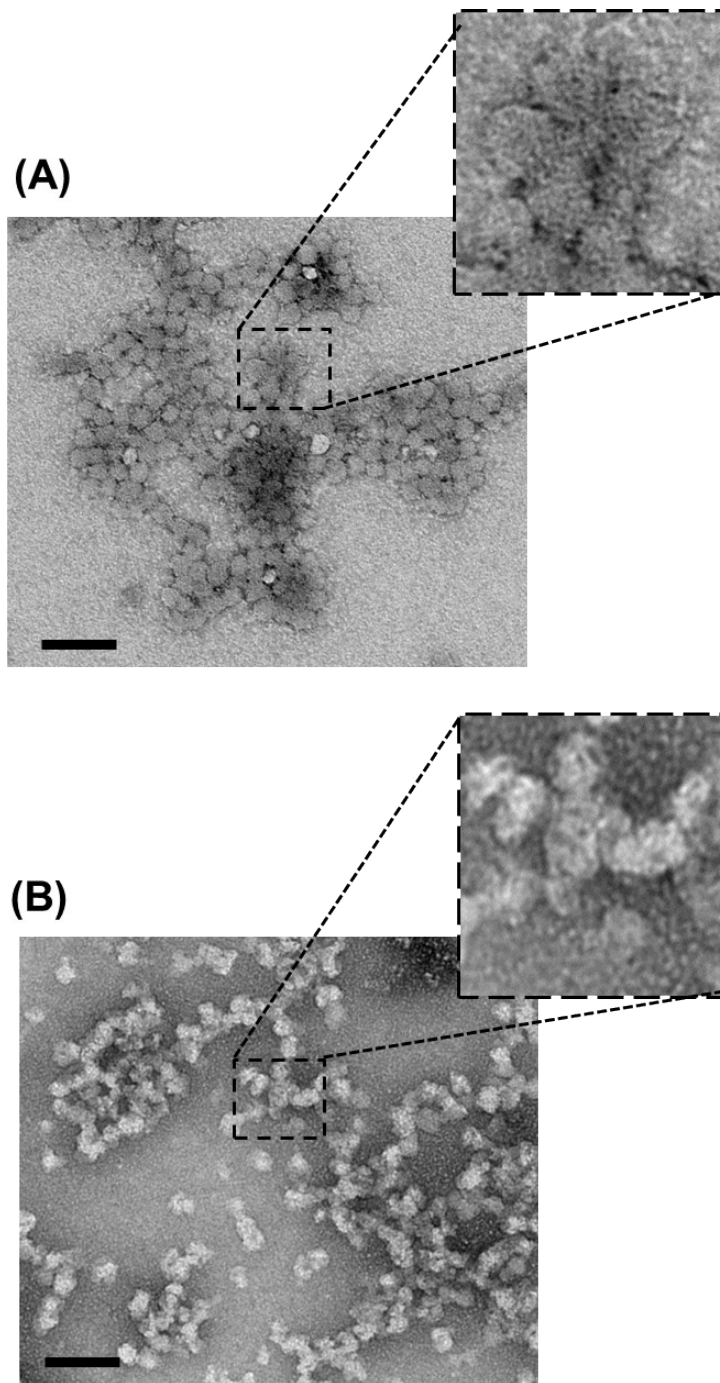


**Figure S12.** TEM images for MG1 after (A) photo-crosslinking at 365 nm and (B) photo-decrosslinking at 254 nm. The data were obtained using deposition at pH 7.4 and 25 °C. The scale bars are 100 nm.

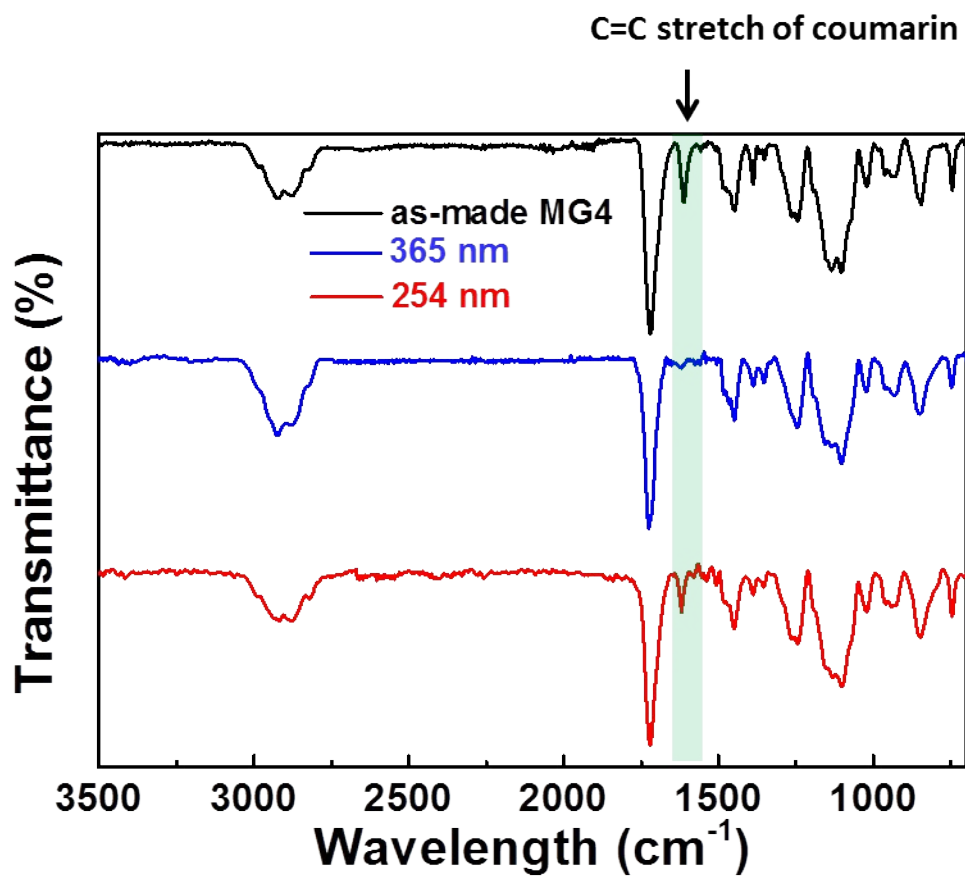


**Figure S13.** FTIR for MG4 before and after photo-crosslinking at 365 nm and photo-decrosslinking at 254 nm. The data was obtained using freeze-dried samples. The green band shows the C=C band at 1620  $\text{cm}^{-1}$ .



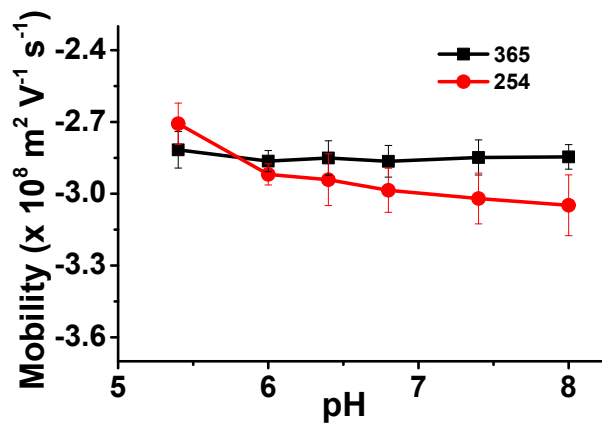


**Figure S14.** Variation of electrophoretic mobility with pH for MG4 at 25 °C when photo-crosslinked (365 nm irradiation) or photo-de-crosslinked (254 nm).

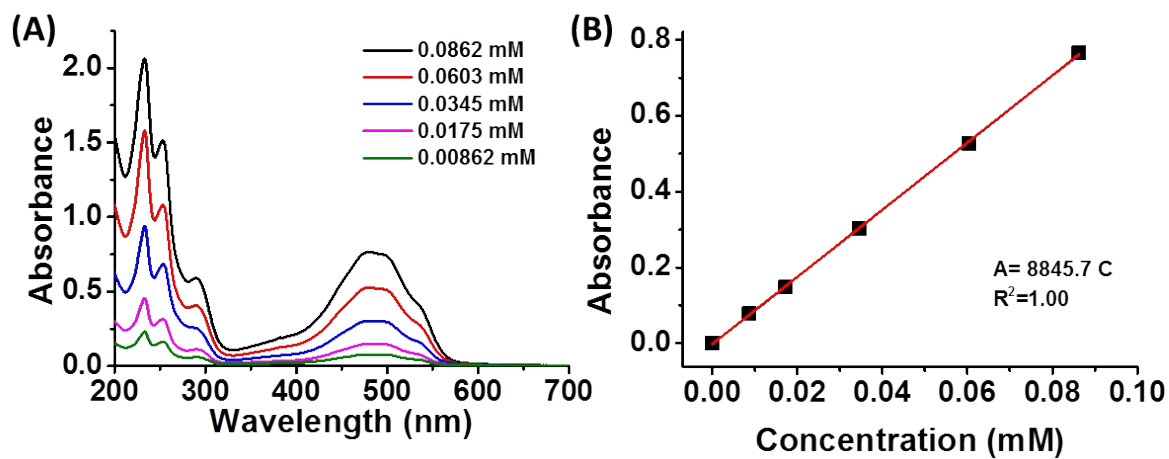


**Figure S15.** (A) UV-visible spectra for DOX at various concentrations. (B) Variation of absorbance at 480 nm with DOX concentration. The molar extinction coefficient was calculated from (B) as  $8845.7 \text{ mol}^{-1} \text{ dm}^3 \text{ cm}^{-1}$ .

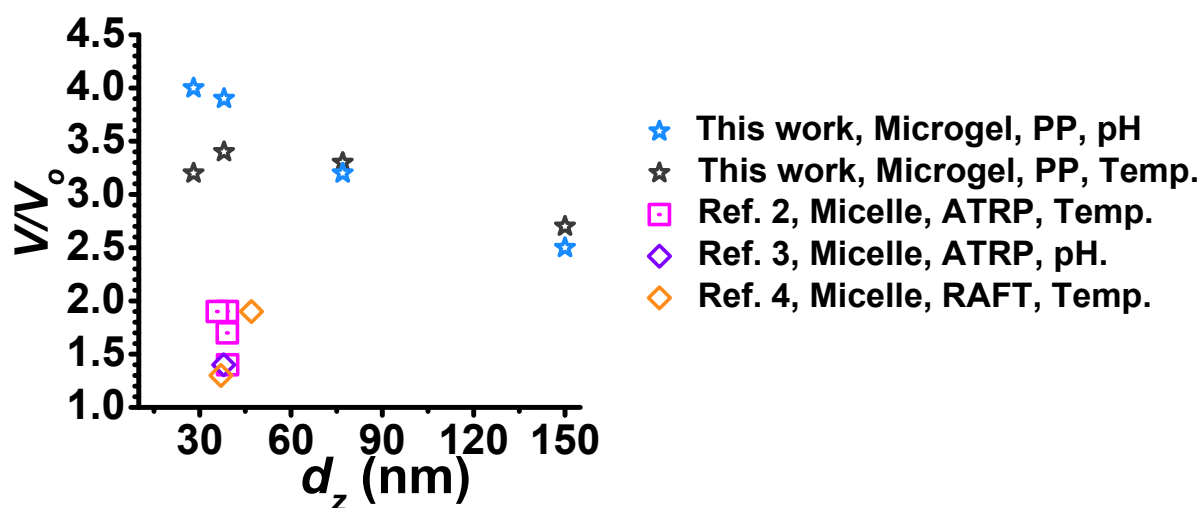


**Figure S16.** Volume ratios ( $V/V_0$ ) for MG1 to MG4 and those from studies on related CMA-nanoparticles. The data from this study were measured using (blue stars) variable pH at 25 °C or (black stars) variable temperature at pH 6.0. PP refers to precipitation copolymerisation. The  $d_z$  values were obtained from DLS data for the de-swollen particles (see Table S2).

**Table S1** Comonomer formulations used to prepare the microgels in this study

MG	MEO <sub>2</sub> MA / mol.%	MAA / mol.%	CMA / mol.%	Total mass/g <sup>a</sup>
MG1	66.0	24.0	10.0	1.35
MG2	66.0	24.0	10.0	1.80
MG3	65.5	24.5	10.0	0.24
MG4	60.4	23.6	15.9	0.24

<sup>a</sup> Total mass of monomers.

**Table S2.** Volume ratios of particles in this work as well as other studies.

Diameter/ nm <sup>a</sup>	$V/V_o$ <sup>b</sup>	Responsive behaviours		Reference
		pH	Temperature	
39	1.9		√	3
36	1.9		√	3
39	1.7		√	3
39	1.4		√	3
38	1.4	√		4
47	1.9		√	5
37	1.3		√	5
28	4.0	√		This work
	3.2		√	
39	3.9	√		This work
	3.4		√	
77	3.2	√		This work
	3.3		√	
150	2.5	√		This work
	2.7		√	

<sup>a</sup> Diameters obtained from DLS data for the de-swelling particles.

<sup>b</sup>  $V/V_o$  represents the ratio of the volumes determined from the diameters determined from DLS before ( $V_o$ ) and after ( $V$ ) photo-de-crosslinking.

**References**

1. M. H. Smith, E. S. Herman and L. A. Lyon. *J. Phys. Chem. B* 2011, **115**, 3761-3764.
2. J. Q. Jiang, B. Qi, M. Lepage and Y. Zhao. *Macromolecules* 2007, **40**, 790-792.
3. J. He, X. Tong and Y. Zhao. *Macromolecules* 2009, **42**, 4845-4852.
4. Q. A. Jin, G. Y. Liu and J. A. Li. *Eur. Polym. J.* 2010, **46**, 2120-2128.
5. J. He, B. Yan, L. Tremblay and Y. Zhao. *Langmuir* 2011, **27**, 436-444.